MICROCONTROLLER-BASED DATA LOGGING INSTRUMENTATION SYSTEM FOR WIND SPEED AND DIRECTION MEASUREMENTS

D. W. Wekesa, J. N. Mutuku and J. N. Kamau
Department of Physics, Jomo Kenyatta University of Agriculture and Technology, Nairobi
E-mail: davwekesa2009@yahoo.com

Abstract
In this study, a microcontroller based data logger for measuring wind speed and wind direction has been designed. The designed system uses the Atmel microcontroller family which consists of sensor inputs, a microcontroller and a data storage device. The system was designed and developed to measure the wind speed and direction with the help of anemometer and wind vane sensors respectively. The results were stored in an Electrically Erasable Programmable Read Only Memory (EEPROM) for post process analysis. The collected data were transmitted to a PC through an RS-232 serial interface, and were processed using the 208W Data logger support software. Wind speed and direction measured by the microcontroller-based data logging system were analyzed using line graphs, scatter correlation charts and wind roses. Wind speeds were measured at 9.00 a.m, 12.00 noon and 5.00 p.m using fabricated sensors and also at JKUAT meteorological station. The correlation indices of microcontroller–based data logger instrumentation system data and JKUAT meteorological data were determined. The correlation indices for the corresponding three times were calculated as 0.997, 0,997 and 0.999 respectively. Thus the wind speed measured by the fabricated sensor was found to correlate strongly to the to the JKUAT Meteorological datasheet. Wind rose analysis revealed that the wind direction was fairly consistent from between 180^0 and 170^0 which is generally from South to South-east for the months of August and September.

Key words: Microcontroller, anemometer and wind vane sensors, data logger

1.0 Introduction

Natural resources are running out and the cost of electricity alone has more than doubled in the past year (Kamau et al., 2010). Although the wind power, which is one of the most attractive way to produce electrical energy, has been used for many years in United States (US), Russia, Denmark, Great Britain, Turkey, and Western Germany (Engstrom, 2009; Haci and Vedat, 2007), use of this energy has increased recently in Kenya. Therefore, there is need to develop alternative energy sources such as wind energy to satisfy the growing demand without harming the environment using accurate devices.

Wind speed and wind direction sensing and recording on a continuous basis is required for many applications such as air and water navigations, wind power generating plants, agricultural institutions by farmers among others. Determination of wind speed and direction is very important for weather forecasting and air and water navigation (Olaleye, 2002). In general, constant wind direction and low to moderate wind velocity indicate a stable air mass and thus fair weather. High wind velocity along with variable wind direction, on the other hand, indicates an unstable weather.

A common type of anemometer measures the wind speed by means of a set of three cups which rotate on a vertical axis. The force of the wind on the cups causes them to rotate at a speed which is proportional to the speed of the wind. Thus the greater the wind the faster the rotation of the cups. By rotating the anemometer, a sine wave is produced whose frequency proportionally changes with the wind speed.

One of the most important factors for installing a wind power system is to choose the site where the system will be installed. It will be uneconomical to build wind power system without investigating wind potential of the site. The period of return on investment is another important factor, even if the wind power potential is satisfactory (Haci and Vedat, 2007).

Therefore, this study aimed at designing a microcontroller based data logging instrumentation system for wind speed and direction measurements; and analyzing wind speeds and determining the correlation indices of microcontroller-based data logger instrumentation system data and JKUAT meteorological data.

2.0 Materials and Methods

2.1 Fabrication of Anemometer Sensor

The anemometer sensor used in this study was fabricated by use of a transparent disk (Kevin, 2008). The disk, which is mounted on the rotating shaft, has patterns of opaque and transparent sectors coded into an incremental disk as shown in Figure 1.

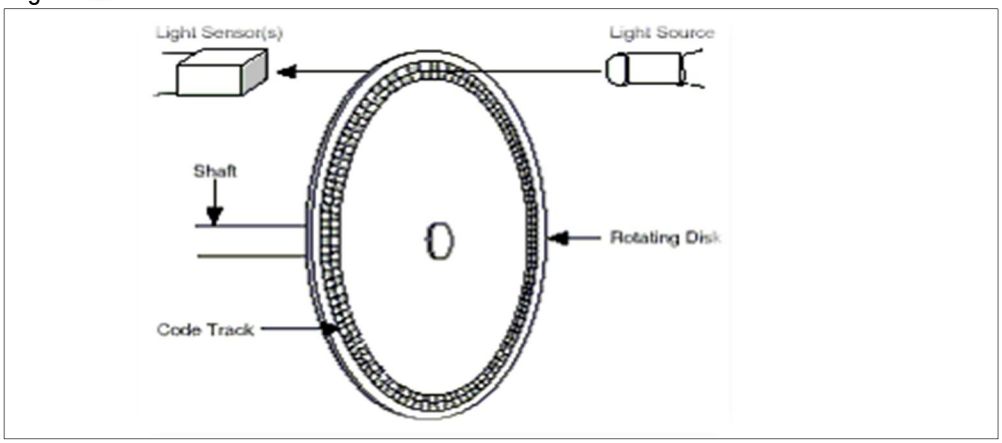

Figure 1: Incremental encoder (Patil, 2008)

As the disk rotates, these patterns interrupt the light emitted onto the photo detector, generating a pulse signal output. The output signal is fed into an incremental encoder which generates a pulse for each incremental step in its rotation. The striking air molecules exert a force on the anemometer cups (illustrated in Plate 1) causing the shaft to rotate about its axis. As the air velocity increases, the anemometer shaft's rotational velocity increases proportionately. The output of incremental encoder is a pulse signal that is generated when the transducer disc rotates. The signals were fed to Atmega32 microcontroller which determined both angular displacement and angular velocity by counting the pulses or by timing the pulse width using a clock signal.

Plate 1: The anemometer sensor fitted with cups

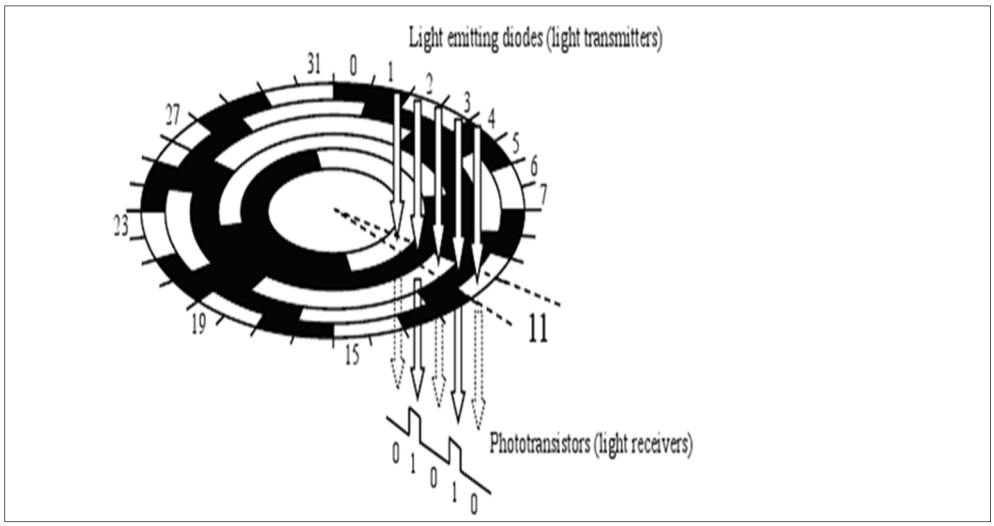

2.2 Fabrication of Wind Vane Sensor

Wind direction is measured by use of wind vanes. The wind vane sensor was fabricated by use of an absolute optical encoder with peripheral track that was connected to the shaft being measured (Patil, 2008). The disc was placed between the light source and the phototransistor which is a light receiver as shown in Figure 2.

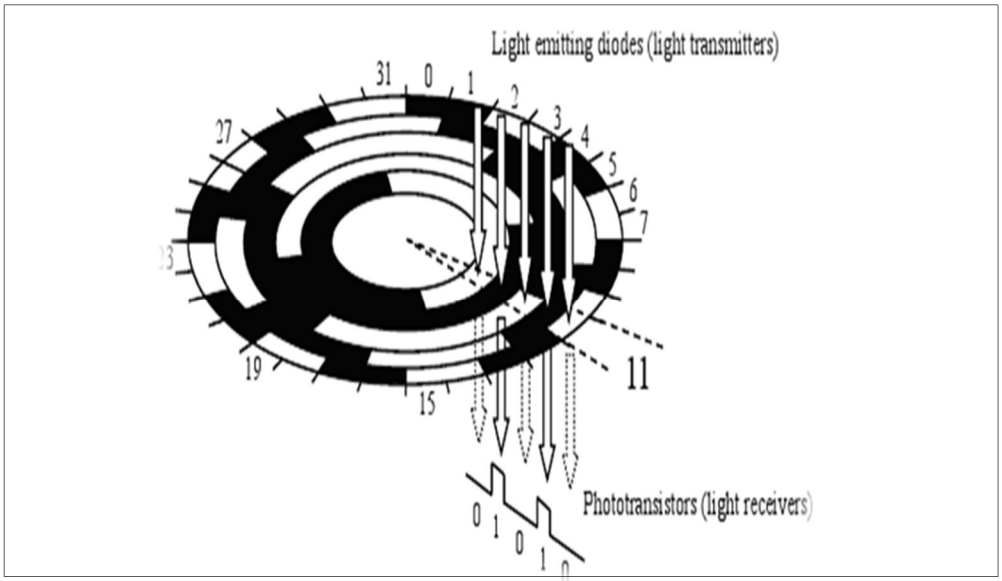

Figure 2: Digital angle-encoder disk (5-bits) (Patil, 2008)

A pulse of light from the Light Emitting Diode (LED) strikes the phototransistor every time a slot on the disk is aligned between them to measure absolute position. The absolute encoder used had five tracks representing a 5-bit binary

number. Each track required a separate set consisting of an LED and a phototransistor sensor, and produced a binary digit. By using five digits, the binary count of 00000 to 11111, it was possible to represent numbers 0 - 31. Each number represents a section of equal size, the encoder disk being divided into thirty two, 11.25-degree sections. With standard binary numbers, it is common to have more than one digit change simultaneously, so a Gray code binary system was used for the absolute optical encoder. The conversion circuit based on the Atmega32 microcontroller was used to convert the Gray code to natural binary for use by the personal computer.

The advantage of Gray code was that if a bit changed too soon or too late, the error produced was insignificant because it was less than one degree, and never indicated a zone more than one section away. The angle was represented by 5 bits; and its resolution was as follows (Kevin, 2008):

$$\frac{360}{2^n} \quad \text{..... (1)}$$

where n is the number of bits.

A weighted pointer was connected to a small flat plate of the wind vane to reduce damping effects as shown in Plate 2. The exposed parts were made of anodized aluminum and stainless steel suitable for permanent weather exposure.

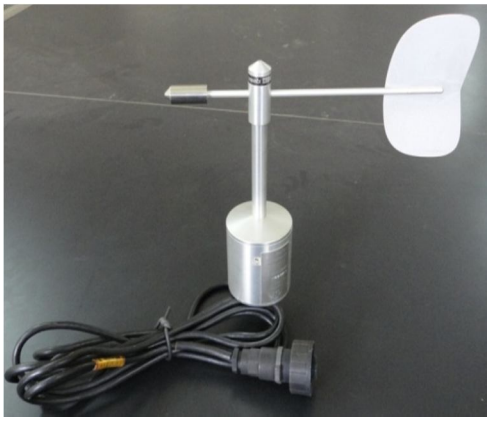

Plate 2: The wind vane sensor connected with weighted pointer

2.3 Wind Profile Power Law

The wind profile power law is a relationship between the wind speeds at one height, and those at another. The power law is often used in wind power

assessments where wind speeds at the height of a turbine must be estimated from near surface wind observations, or where wind speed data at various heights must be adjusted to a standard height prior to use. The wind profile power law relationship is of the form (Lu et al., 2002):

$$\frac{v_2}{v_1} = \left(\frac{h_2}{h_1}\right)^{\alpha} \quad \text{..... (2)}$$

where v2 is the wind speed (in km/h) at height h2 measured in meters, and v1 is the known wind speed at a reference height h1. The exponent (α) is an empirically derived coefficient that varies dependent upon the stability of the atmosphere.

2.4 Wind Roses

A wind rose is a graphic tool used to give a succinct view of how speed and direction of wind are typically distributed at a particular location. It is a polar plot that represents the percentage of the time that the wind direction falls within the sector of the compass and when presented in a circular format, the modern wind rose shows the frequency of winds blowing from particular directions (Kamau et al., 2010).

The length of each "spoke" around the circle is related to the frequency that the wind blows from a particular direction per unit time. Each concentric circle represents a different frequency, emanating from zero at the center to increasing frequencies at the outer circles. A wind rose plot may contain additional information, in that each spoke is broken down into colour-coded bands that show wind speed ranges. Wind roses typically use 16 cardinal directions which may be subdivided into as many as 32 directions. In terms of angle measurement in degrees, North corresponds to 0°/360°, East to 90°, South to 180° and West to 270°. This can be summarized in the graduation direction in Table 1.

Table 1: Wind graduation direction table

Abbrev.	Wind Dir	Degrees(0)
N	North	0/360
NNE	North-northeast	22.5
NE	North-east	45
ENE	East-northeast	67.5
E	East	90
ESE	East-southeast	112.5
SE	South-east	135
SSE	South-southeast	157.5
S	South	180
SSW	South-southwest	202.5

SW	South-west	225
WSW	West-southwest	247.5
W	West	270
WNW	West-northwest	292.5
NW	North-west	315
NNW	North-northwest	337.5

Source: Sathyajith (2006)

3.0 Results and Discussion

In this study, the wind speed was calculated and recorded in km/h by the microcontroller based data logging system fed with the cup anemometer sensor. Wind direction was measured using a wind vane. The vane constantly sought a position of force equilibrium by aligning itself with the wind direction. The wind vanes in this paper used a digital transducer that produced electrical signals relative to the position of the vane. This was done at 9.00 a.m, 12.00 noon and 5.00 p.m daily starting from August 1st 2011 for a period of six weeks.

3.1 Wind Speed Output

Figure 3 shows wind speed output graphs for experimental data, extrapolated data and JKUAT meteorological data collected daily at 9.00 a.m starting from August 1st 2011 for a period of six weeks.

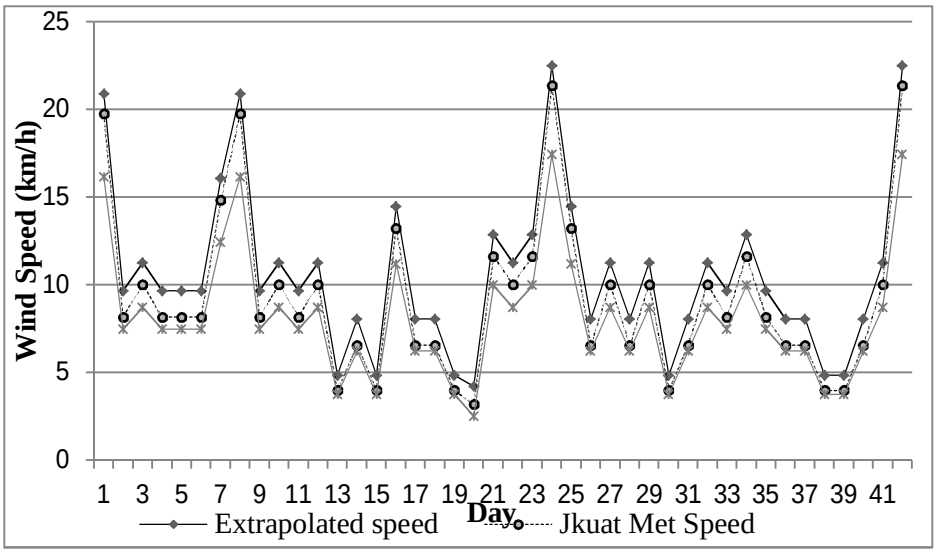

Figure 3: Wind speed profile from 1st August to 11th September at 9.00 a.m

Figure 3 represents three graphs for wind speed in km/h which include extrapolated speed, JKUAT meteorological speed and experimental speed. The

extrapolated speed is obtained from that of experimental speed by use of the wind profile power law relationship at a height of 10 m (Eq. 2) which is the universally standard meteorological measurement height (Benghanen, 2009). From Figure 3, the JKUAT meteorological speed graph was slightly lower than the extrapolated speed graph. This is due to the minimal mechanical friction and improved measuring technique by the data logging system.

The correlation scatter chart for wind speed data at 9.00 a.m (at a height of 10 m) was plotted and corresponding correlation index obtained as shown in Figure 4.

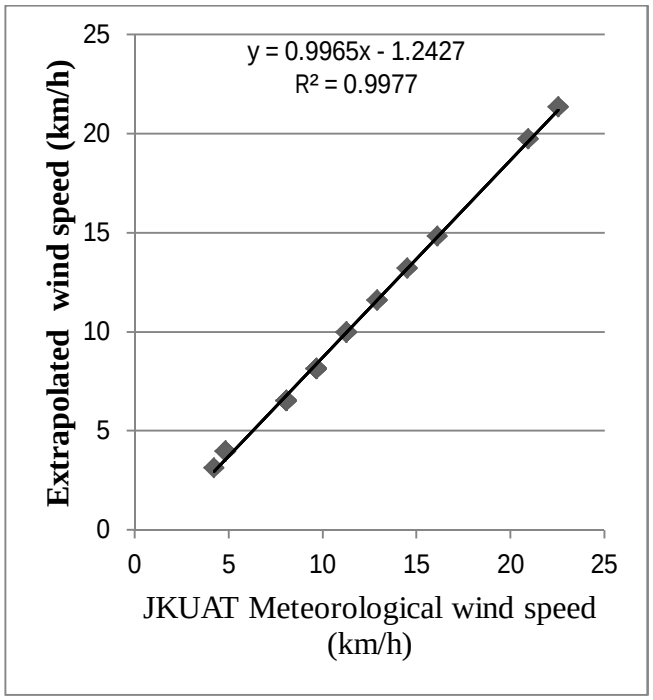

Figure 4: Correlation Chart for wind speed data at 9.00 a.m (1st August-11th September)

The extrapolated wind speed (y-axis) and the JKUAT meteorological wind speed (x-axis) were correlated by the equation:

$$y = 0.996x - 1.24 \quad \text{.....(3.1)}$$

The corresponding correlation index R2 was 0.997 and the gradient of the correlating equation was close to unity (0.996) implying a strong correlation between experimental data and reference data. The y- intercept was -1.24 i.e. when $x = 0$. Thus when $y = 0$, $x = 1.24$, and JKUAT meteorological wind speed

data should be raised by a constant value of 1.24 to comply with results obtained by the data logging system.

Figure 5 shows wind speed output graphs for experimental data, extrapolated data and JKUAT meteorological data collected daily at 12.00 noon starting from August 1st 2011 for a period of six weeks.

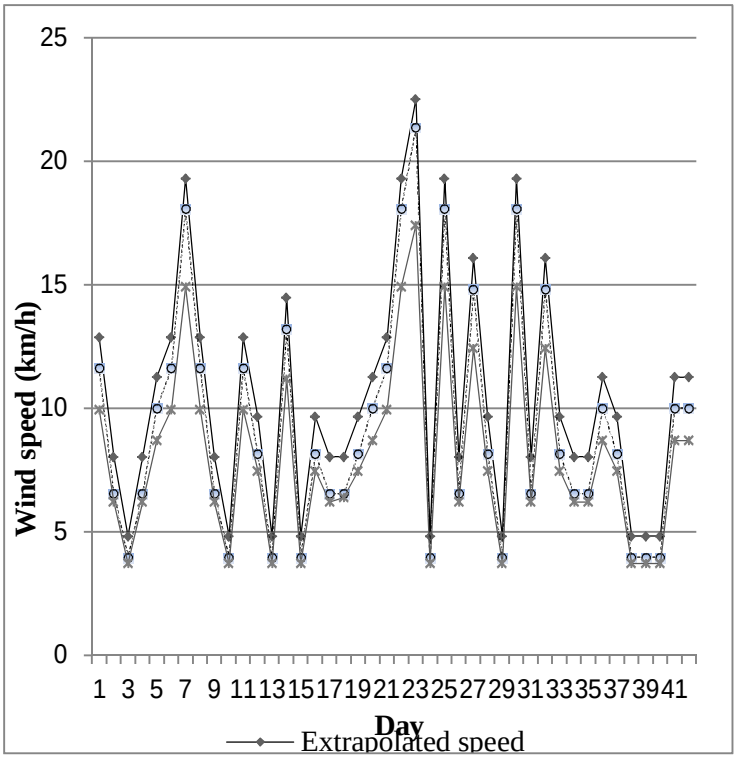

Figure 5: Wind speed profile from 1st August to 11th September at 12.00 noon

From Figure 5, the JKUAT meteorological speed was slightly lower than extrapolated speed as a result of difference in mechanical properties and the measuring techniques by the two rotational anemometers.

The obtained extrapolated wind speed (y-axis) and the JKUAT meteorological wind speed (x-axis) at 12.00 noon were correlated by the equation:

$$y = 0.987x - 1.114 \quad \text{.....(3.2)}$$

where 0.987 was the gradient of the equation.

As in Figure 4, the gradient of the correlating equation and correlation index were close to unity implying a strong correlation.

Figure 6 shows the graphs for experimental, extrapolated and JKUAT Meteorological output wind speed measurements at 5.00 p.m starting from August 1st 2011 for a period of six weeks.

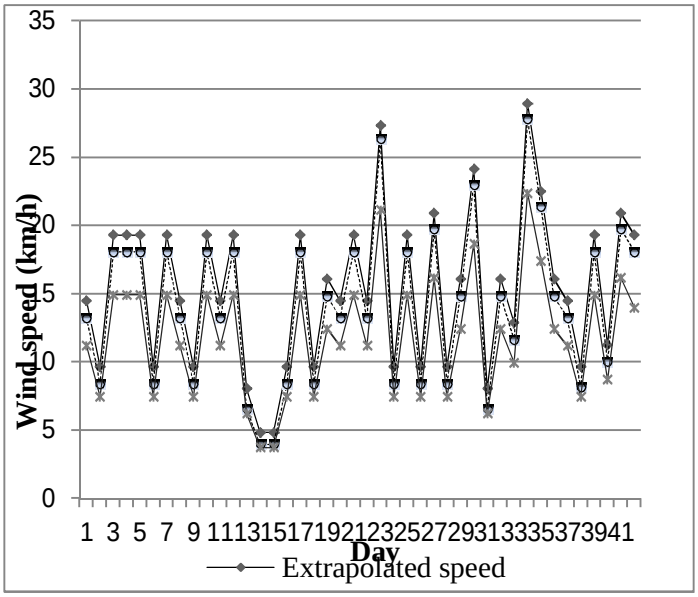

Figure 6: Wind speed profile from 1st August to 11th September at 5.00 p.m

From Figure 6, the wind speeds for the three graphs at 5.00 p.m are also represented where the JKUAT meteorological speed graph was slightly lower than the extrapolated speed graph. As in Figures 3 and 5, this behavior can be explained by difference in mechanical properties and the measuring techniques by the two rotational anemometers. The JKUAT's meteorological rotational anemometer has its shaft directly coupled to an electric generator that generates a.c voltage whose magnitude is directly proportional to the shaft's frequency of rotation. A precision rectifier and a filter are used to convert the a.c voltage generated to d.c voltage that is then directly displayed on a voltmeter calibrated to wind speed. The generated a.c voltage is coil dependent and needs to be calibrated frequently hence its performance is not very stable and reliable for large variation of wind speeds. This anemometer is faced with mechanical friction and speed limit associated with mechanical properties due to its many parts in contact. However, the rotational anemometer with optical sensors has minimal physical contact with

the shaft reducing the hazard of friction and improving the speed limit as they can respond to a shaft rotating at any practically possible speed. Therefore in general, the JKUAT meteorological speed is slightly lower than the extrapolated speed as shown in the Figures 3, 5 and 6.

The obtained extrapolated wind speed (y-axis) and the JKUAT meteorological wind speed (x-axis) at 5.00 p.m were correlated by the equation:

$$y = 1.003x - 1.275 \quad \text{.....(3.3)}$$

where 1.003 is the gradient of the equation.

The correlation index R2 (0.999) at 5.00 p.m was almost the same as that obtained for correlation chart for wind speed at 9.00 a.m and 12.00 noon. From Equations 3.1, 3.2 and 3.3, the gradients of their correlation equation and correlation indices were close to unity implying a strong correlation between the two sets of data.

3.2 Wind direction output

Figure 7 shows a wind rose diagram for 2m height at 9.00 a.m in Juja for wind direction output by the data logging instrumentation system for a period of six weeks from 1st August to 11th September 2011.

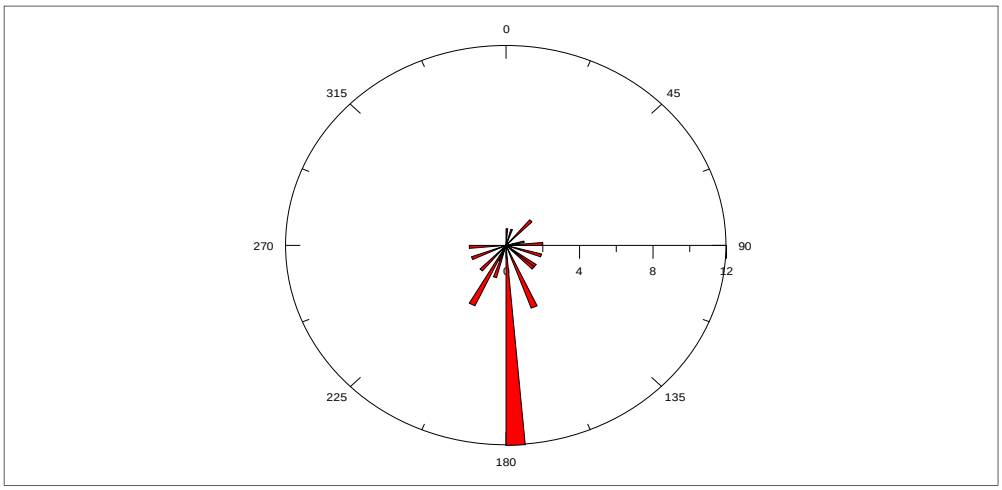

Figure 7: Wind rose diagram for 2 m height at 9.00 a.m in Juja

The length of each "spoke" around the circle relates to the frequency of the wind blowing from a particular direction per unit time. From the wind rose diagram of Figure 7, it was observed that there was high frequency of winds blowing in Juja at 9.00 a.m from the south which formed 40% of the total.

Figure 8 shows a wind rose diagram for 2 m height at 12.00 noon in Juja. Similar to Figure 7, it was observed that there was high frequency of winds blowing in at 12.00 noon from the south.

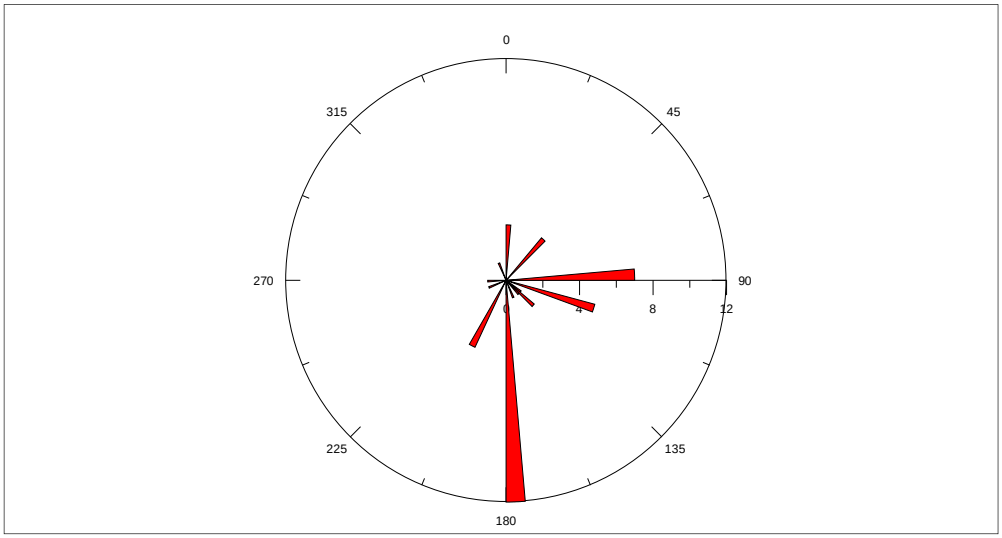

Figure 8: Wind rose diagram for 2m height at 12.00 noon in Juja

Figure 9 shows a wind rose diagram for 2m height at 5.00 p.m in Juja. There was high frequency of winds blowing in Juja at 5.00 p.m ranging from North-east to South-southeast directions.

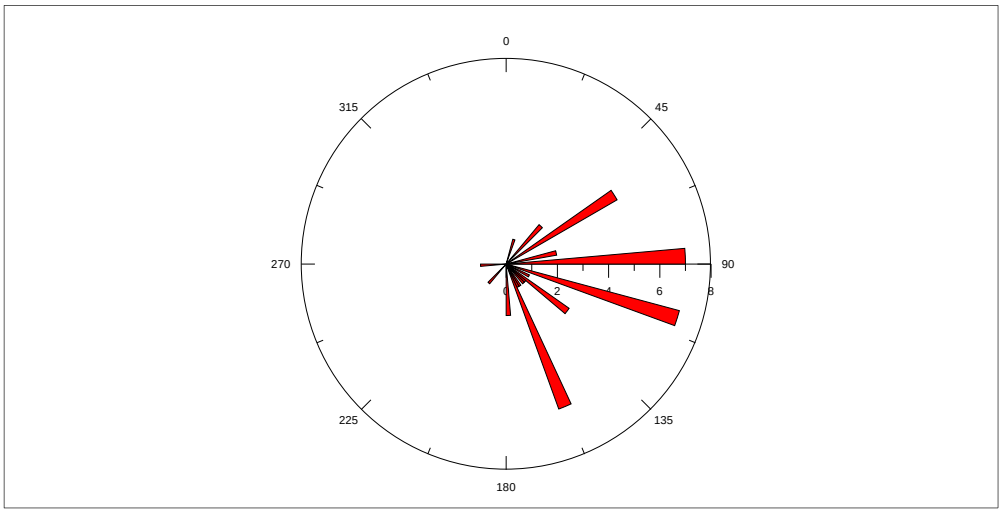

Figure 8: Wind rose diagram for 2 m height at 5.00 p.m

The experimental wind direction measurements were done at height of 2m as opposed to the standard meteorological measurement height of 10m. Generally

there was high frequency of winds blowing from the south at 9.00 a.m and 12.00 noon and from a range of North-east to South-southeast at 5.00 p.m daily from 1st August to 11th September 2011.

4.0 Conclusions

From the plotted line graph charts for wind speed profile, the JKUAT meteorological speed was slightly lower than the corresponding experimental speed as a result of difference in mechanical properties and the measuring techniques by the two rotational anemometers. Therefore, wind measuring techniques and mechanical properties affect the accuracy and hence performance of the wind instrument in use. The correlation indices for the two sets of wind speed data in the morning, midday and evening were 0.997, 0.997 and 0.999 respectively. Thus the wind speed measured by the fabricated sensor was found to correlate strongly to the to the JKUAT Meteorological datasheet. Wind Rose analysis showed that the wind direction was fairly consistent from between 1800 and 1700 which is generally from South to South-east for the months of August and September.

References

Benghanem M. (2009). Measurement of meteorological data based on wireless data acquisition system monitoring. Journal of applied energy. 86, pp 2651 – 2660.

Engstrom S. (2009). Wind energy from a Swedish viewpoint. Journal of royal Swedish academy of sciences. 4, pp 75 – 79

Haci C. and Vedat M. (2007). Multipoint wind speed and direction measurement and data logging by using 8051 – based microcontroller. American journal of science. 157, pp 2482-2488.

Kamau, J.N., Kinyua R. and Gathua J.K. (2010). 6 years of wind data for Marsabit, Kenya average over 14m/s at 100 m hub height: An analysis of the wind energy potential. Renewable Energy. 35, pp 1298-1302.

Kevin L. and Justin D. (2008). Using MA3 absolute shaft encoder to determine wind direction. American journal of science.169, pp 2582-2698.

Lu L., Yang H. and Burnett J. (2002). Investigation on wind power potential on Hong Kong islands - an analysis of wind power and wind turbine characteristics. Renewable Energy. 27, pp 75 – 79.

Olaleye S., Ako N. and Obu D. (2002). Analysis of sky condition using solar radiation data over tropical station, Global journal of pure and applied science. 9, pp 387-392.

Patil M. and Achuthan I. (2008). Wind vane with optical transducer. Journal of applied meteorology. 17, pp 1232 – 1233.

Sathyajith M. (2006). Wind energy: Fundamentals, resource analysis and economics, pp 78-79. Amazon & Co. Ltd, New York.